Supplemental data for:

Delivery of a model lipophilic membrane cargo to bone marrow *via* cell-derived microparticles

Chunyan Yang [1,2,*], Fangfang Chen [1,2,#*], Ping Ren[2], Laren Lofchy[2], Chun Wan[3], Jingshi Shen[3], Guankui Wang[2], Hanmant Gaikwad[2], Craig T. Jordan[4], Robert Scheinman, and Dmitri Simberg[2,#]

[1]*China-Japan Union Hospital of Jilin University, Changchun, Jilin, China*

[2]*The Skaggs School of Pharmacy and Pharmaceutical Sciences, Department of Pharmaceutical Sciences, University of Colorado Anschutz Medical Campus, Aurora, CO, USA*

[3]*Department of Molecular, Cellular and Developmental Biology, University of Colorado Boulder, CO, USA 80309*

[4]*Division of Hematology, Department of Medicine, University of Colorado School of Medicine, Aurora, CO, USA*

*equal contribution

#corresponding authors: dmitri.simberg@cuanschutz.edu, cffemail@163.com

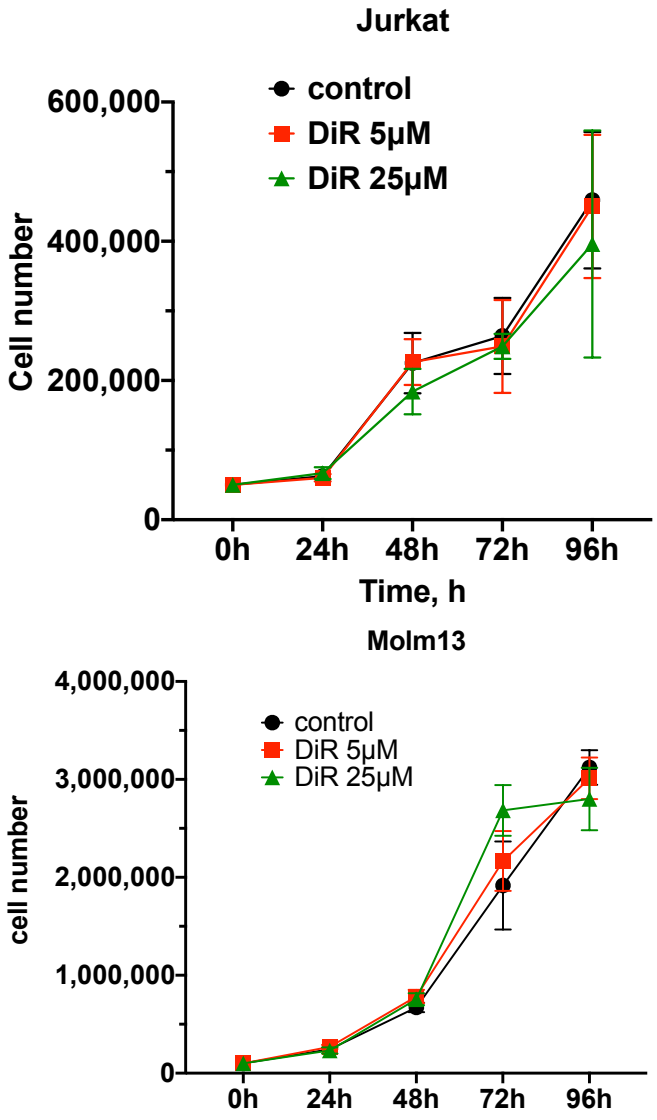

Supplemental Fig. S1: In vitro proliferation curve of non-labeled control and DiR-labeled Jurkat (top) and MOLM13 (bottom) cells

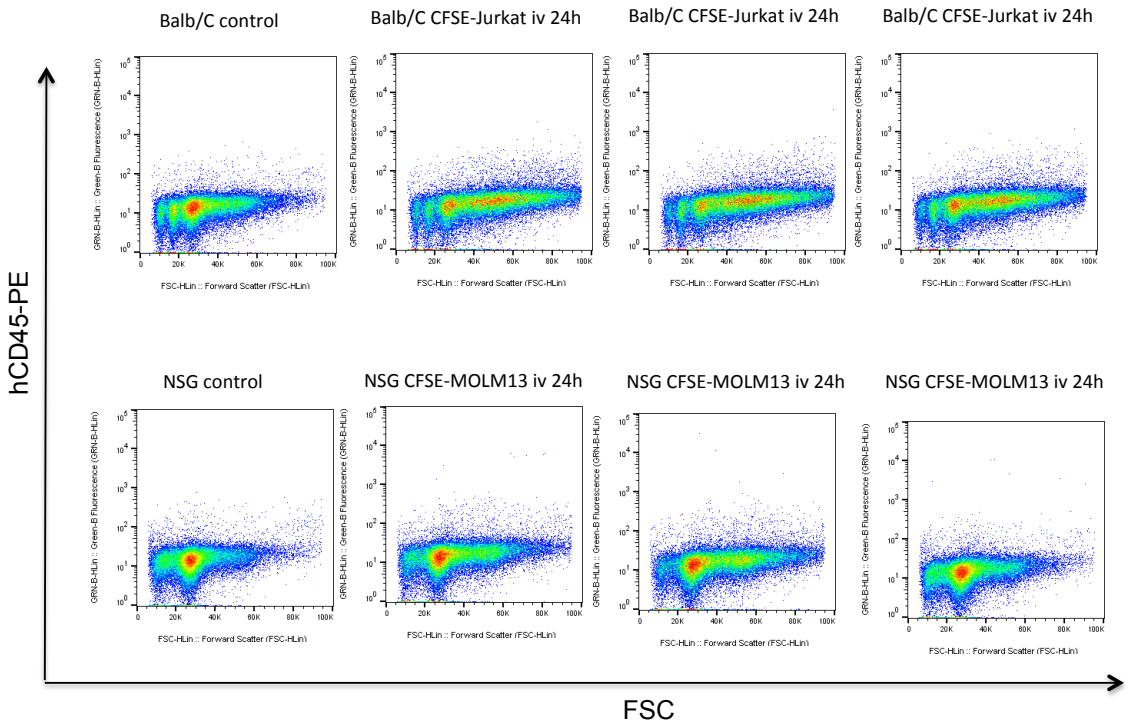

Supplemental Fig. S2: BM Homing of non-labeled MOLM13 and Jurkat cells 24h post injection of 10 million cells/mouse shows less than 0.1% of hCD45+ cells, compared to non-injected control

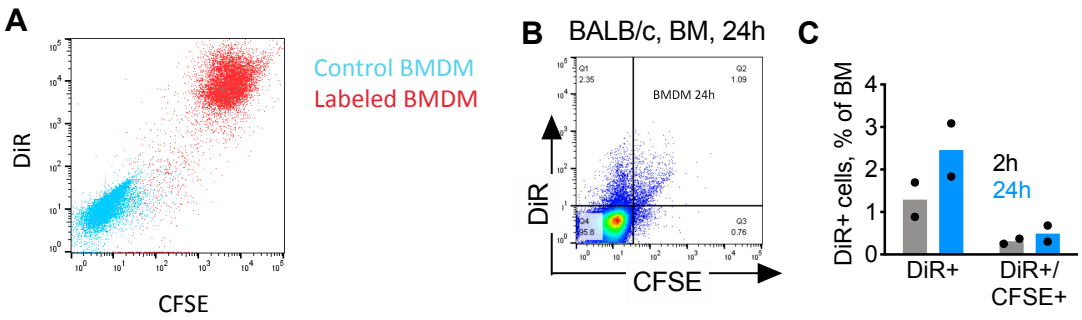

Supplemental Fig. S3: BM homing of bone marrow derived macrophages. A) Labeling of BMDM derived from BALB/c mice. Overlay shows matched populations of unlabeled BMDM and BMDM labeled with 25µM DiR and 10µM CFSE; **B-C**) BM delivery of DiR/CFSE labeled BMDM 24h post injection of 10 million cells per mouse.

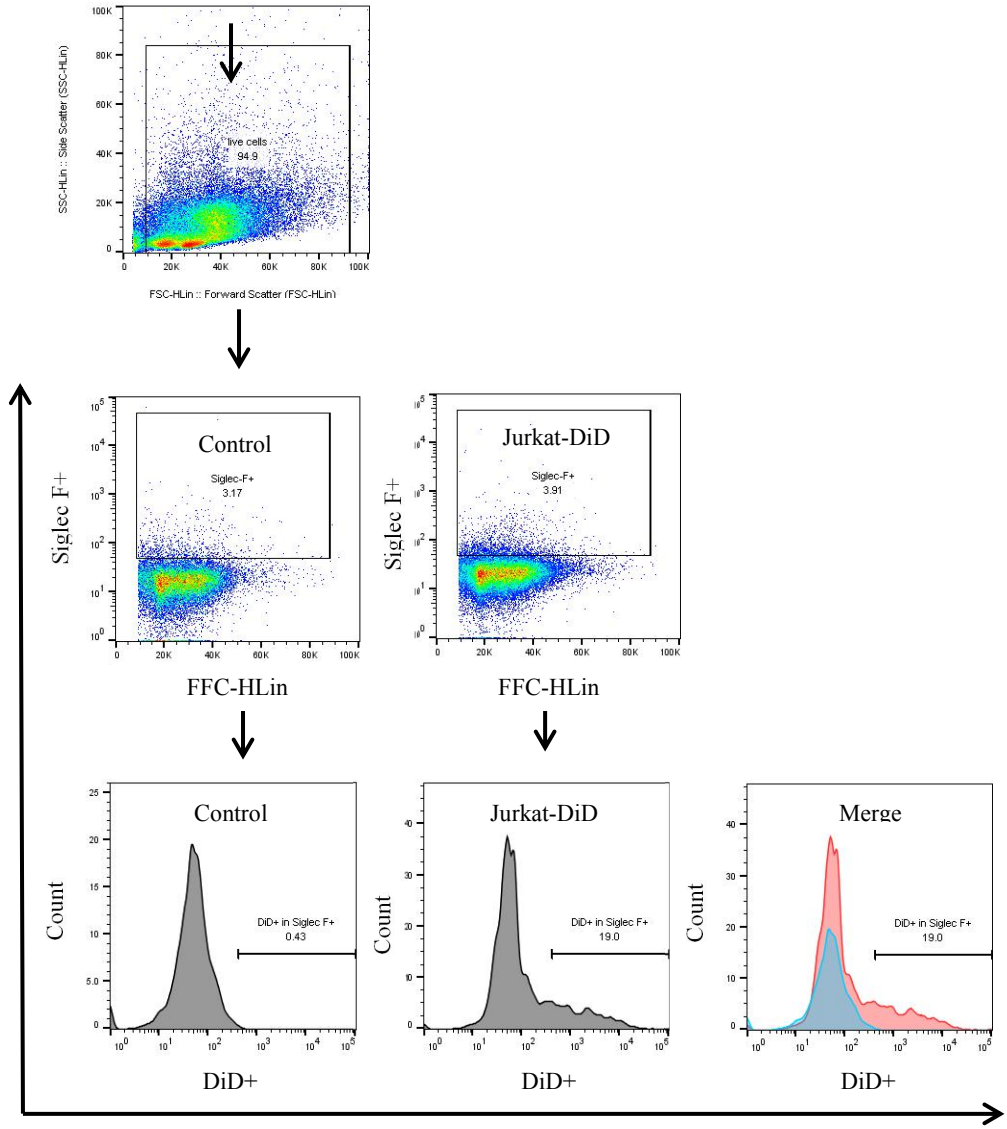

Supplemental Fig. S4. Gating strategy and identification of DiD positive eosinophils in BM 24 after injection of DiD Jurkat in BALB/c mice. Live cells were gated based on SSC-FSC plot (top plot). BM of non-injected (control) and injected mice was compared side by side (middle and lower panel histograms). DiD+ cells were calculated as the difference between control and injected mice (blue histogram, control mice; red histogram, injected mice). The strategy was similar for DiD liposomes. The data are pooled from 3 mice.

.

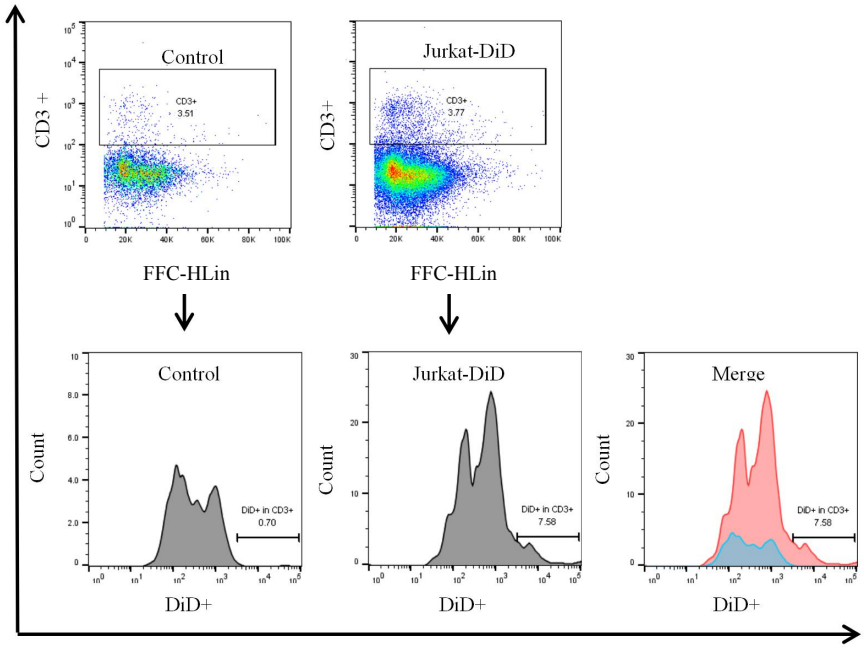

Supplemental Fig. S5: Gating strategy and identification of DiD positive T-cells in BM 24 after injection of DiD Jurkat in BALB/c mice. Please see Fig. S6 for details. The data are pooled from 3 mice.

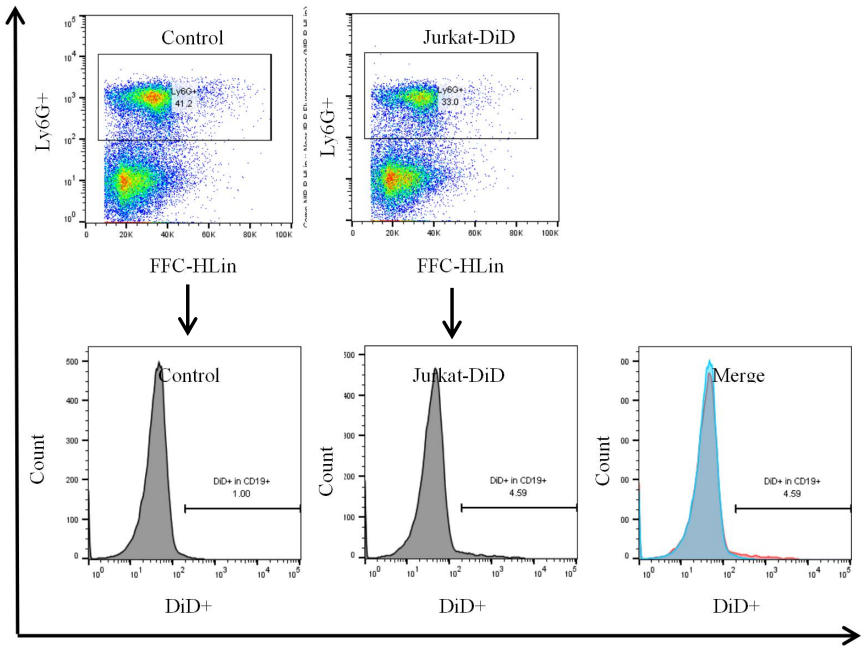

Supplemental Fig. S6: Gating strategy and identification of DiD positive neutrophils in BM 24 after injection of DiD Jurkat in BALB/c mice. Please see Fig. S6 for details. The data are pooled from 3 mice.

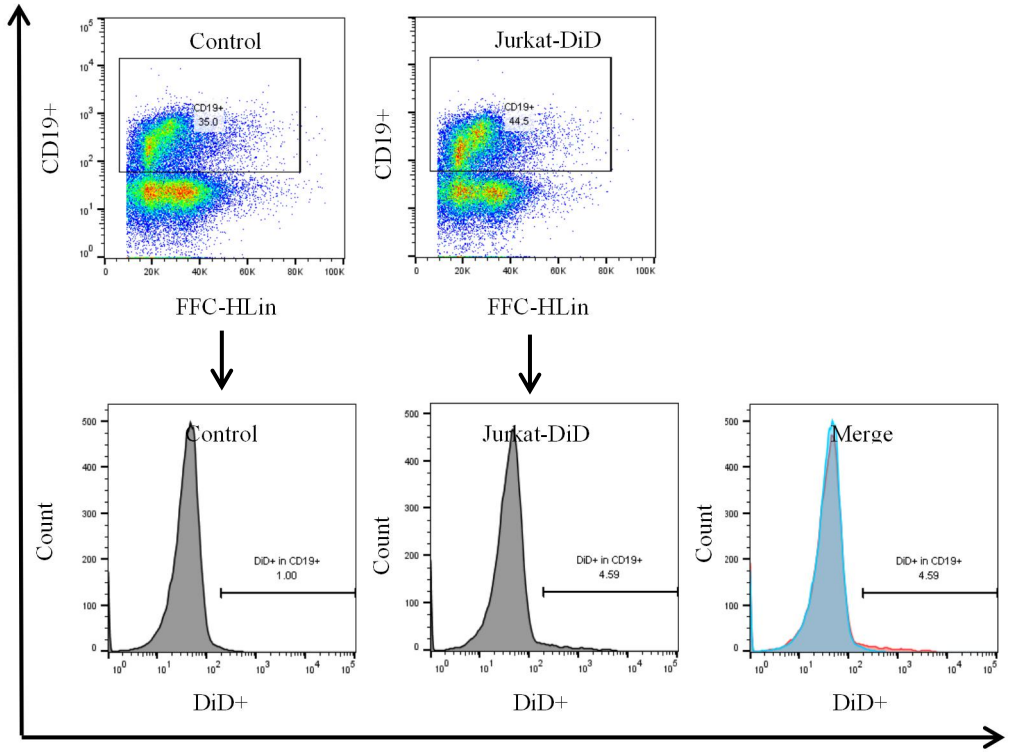

Supplemental Fig. S7: Gating strategy and identification of DiD positive B-cells in BM 24 after injection of DiD Jurkat in BALB/c mice. Please see Fig. S6 for details. The data are pooled from 3 mice.

.

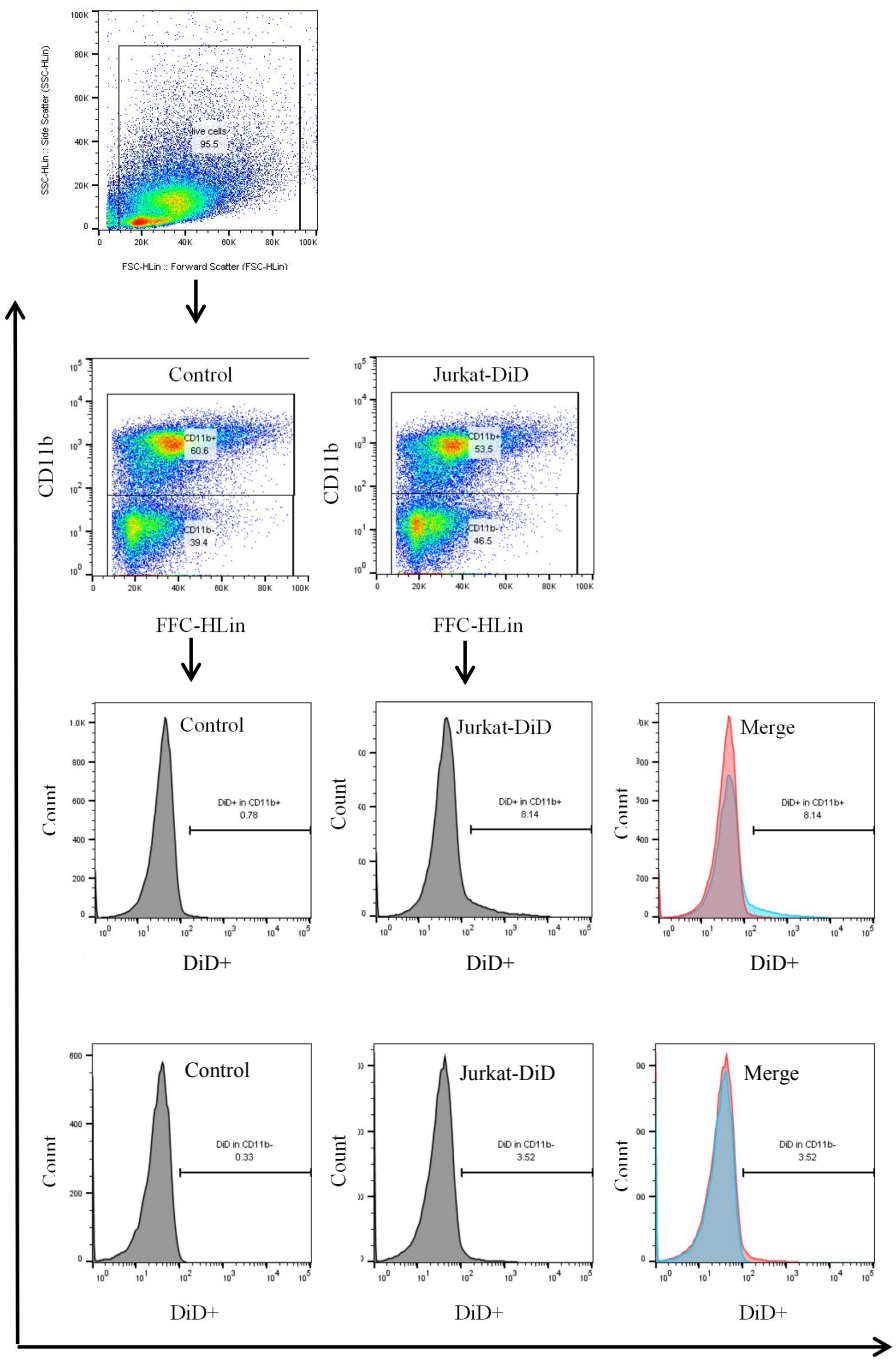

Supplemental Fig. S8: Gating strategy and identification of DiD positive CD11b+ and CD11b- cells in BM 24 after injection of DiD Jurkat in BALB/c mice. Please see Fig. S5 for details. The data are pooled from 3 mice.

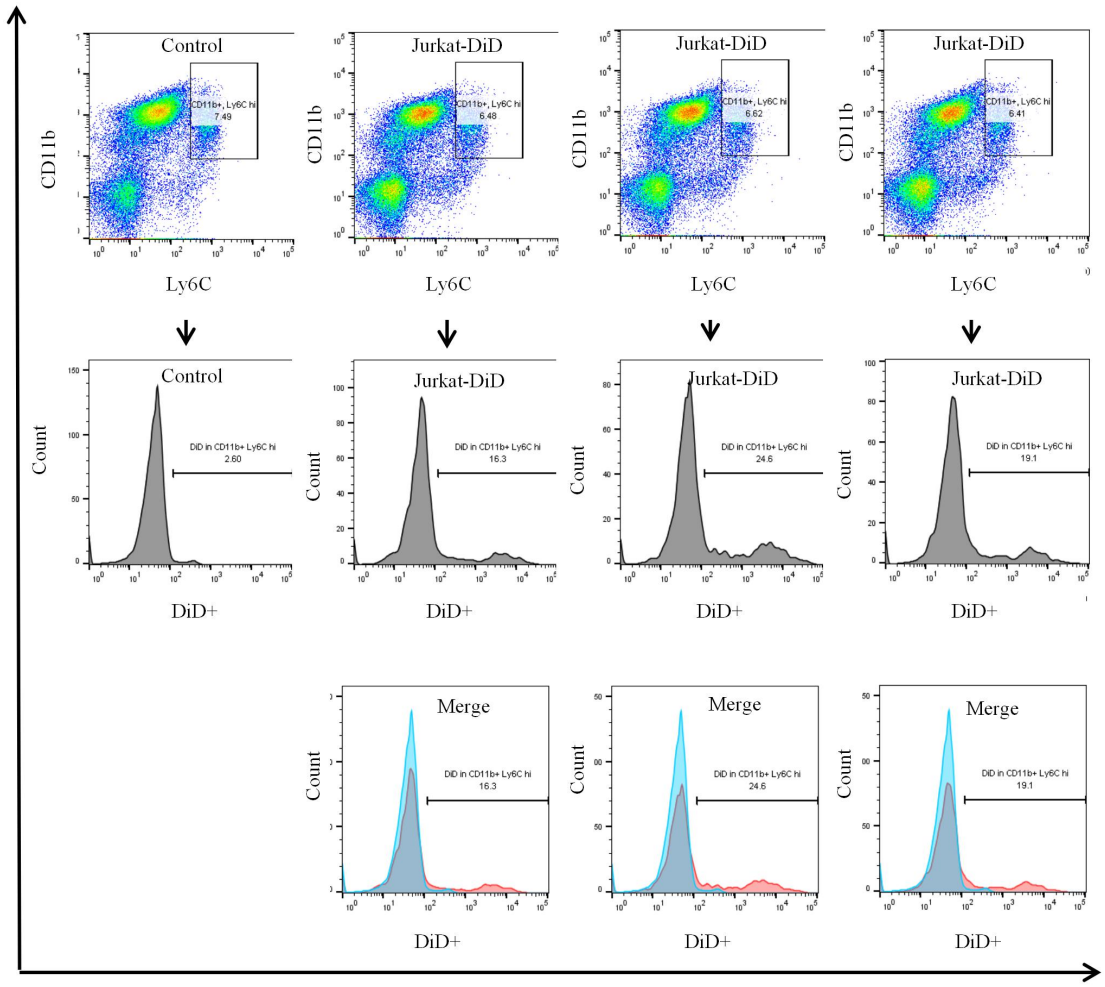

Supplemental Fig. S9. Gating strategy and identification of DiD positive monocytes in BM 24 after injection of DiD Jurkat in BALB/c mice. Live cells were gated based on SSC-FSC plot. BM of non-injected (control) and injected mice was compared side by side (middle and lower panel histograms). DiD+ cells were calculated as the difference between control and injected mice (blue histogram, control mice; red histogram, injected mice). The strategy was similar for DiD liposomes. The data are from 3 mice.

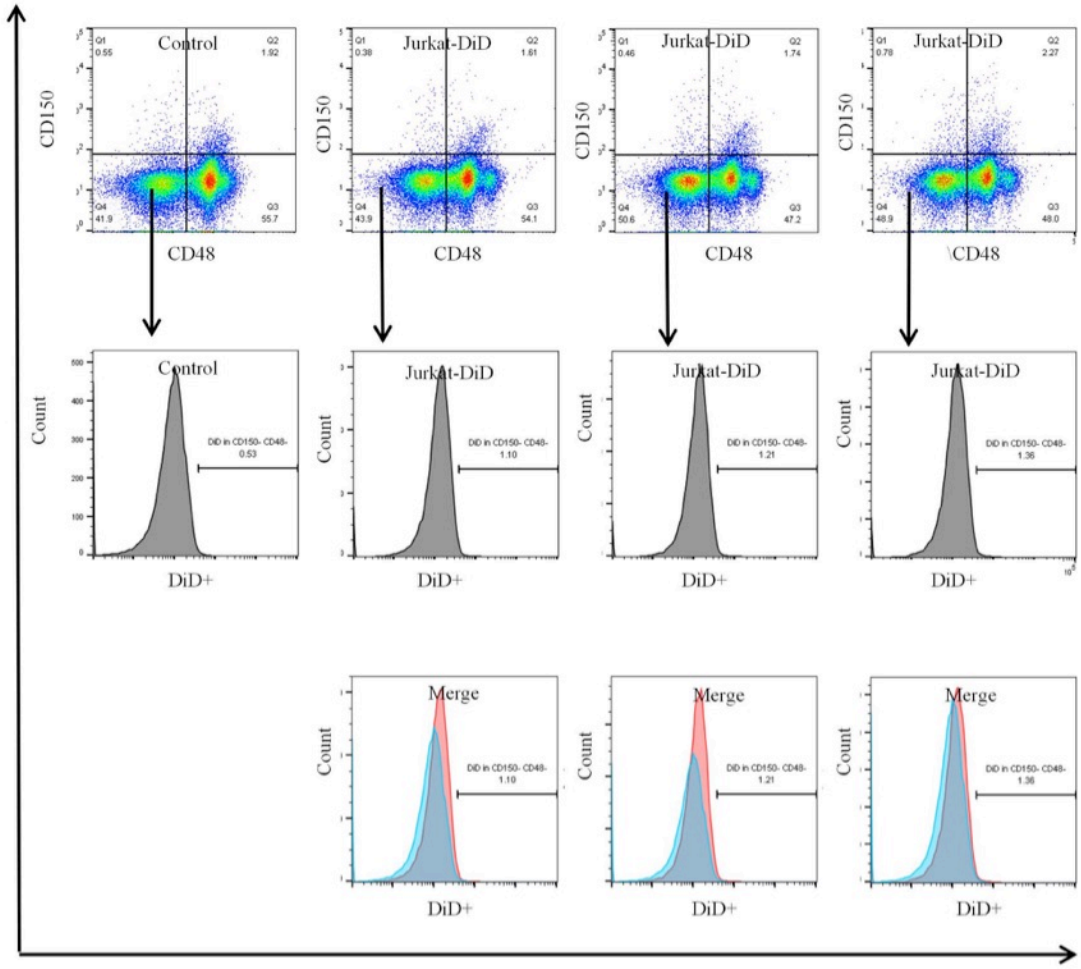

Supplemental Fig. S10. Gating strategy and identification of DiD positive multipotent

progenitors in BM. Please see Fig. S10 for details. The data are from 3 mice.

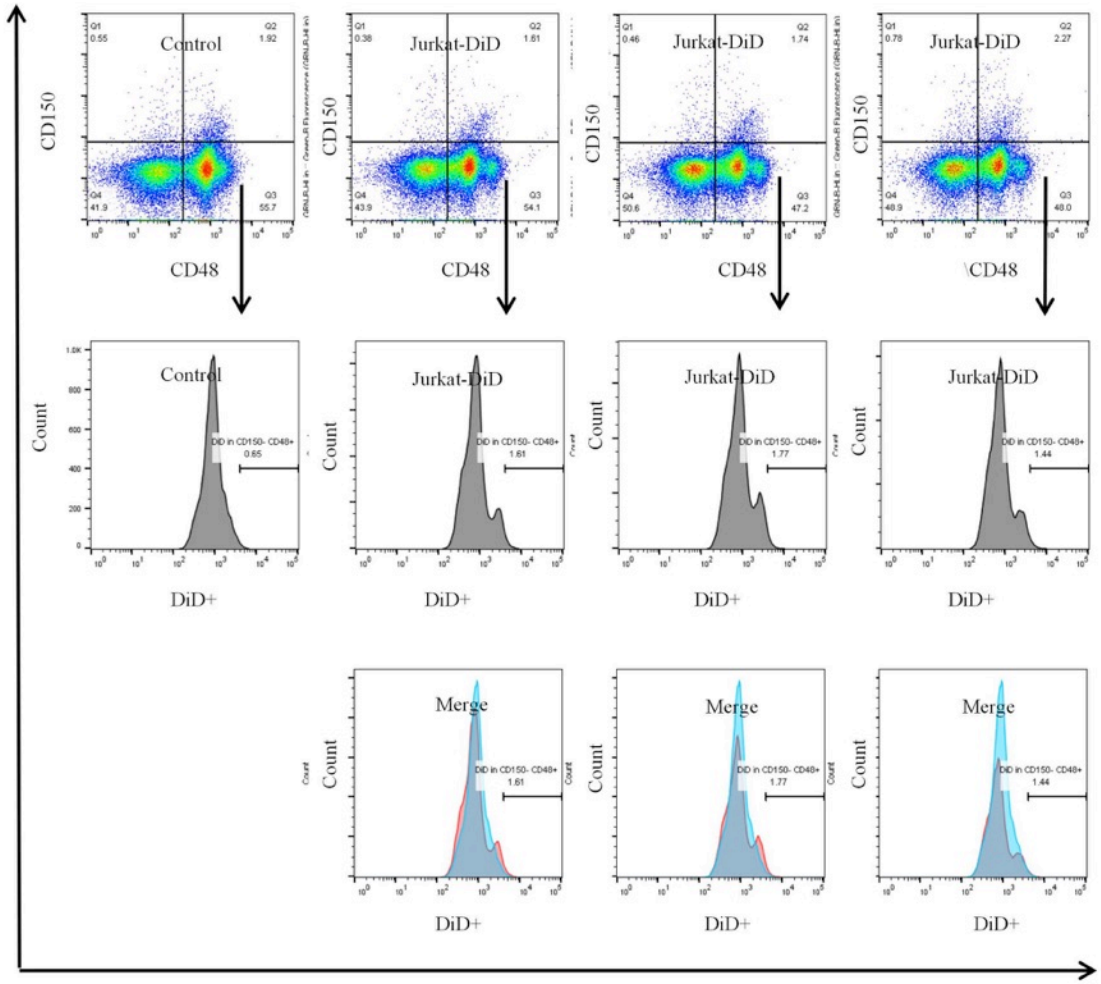

Supplemental Fig. S11. Gating strategy and identification of DiD positive hematopoietic progenitors HPC1 in BM. Please see Fig. S10 for details. The data are from 3 mice.

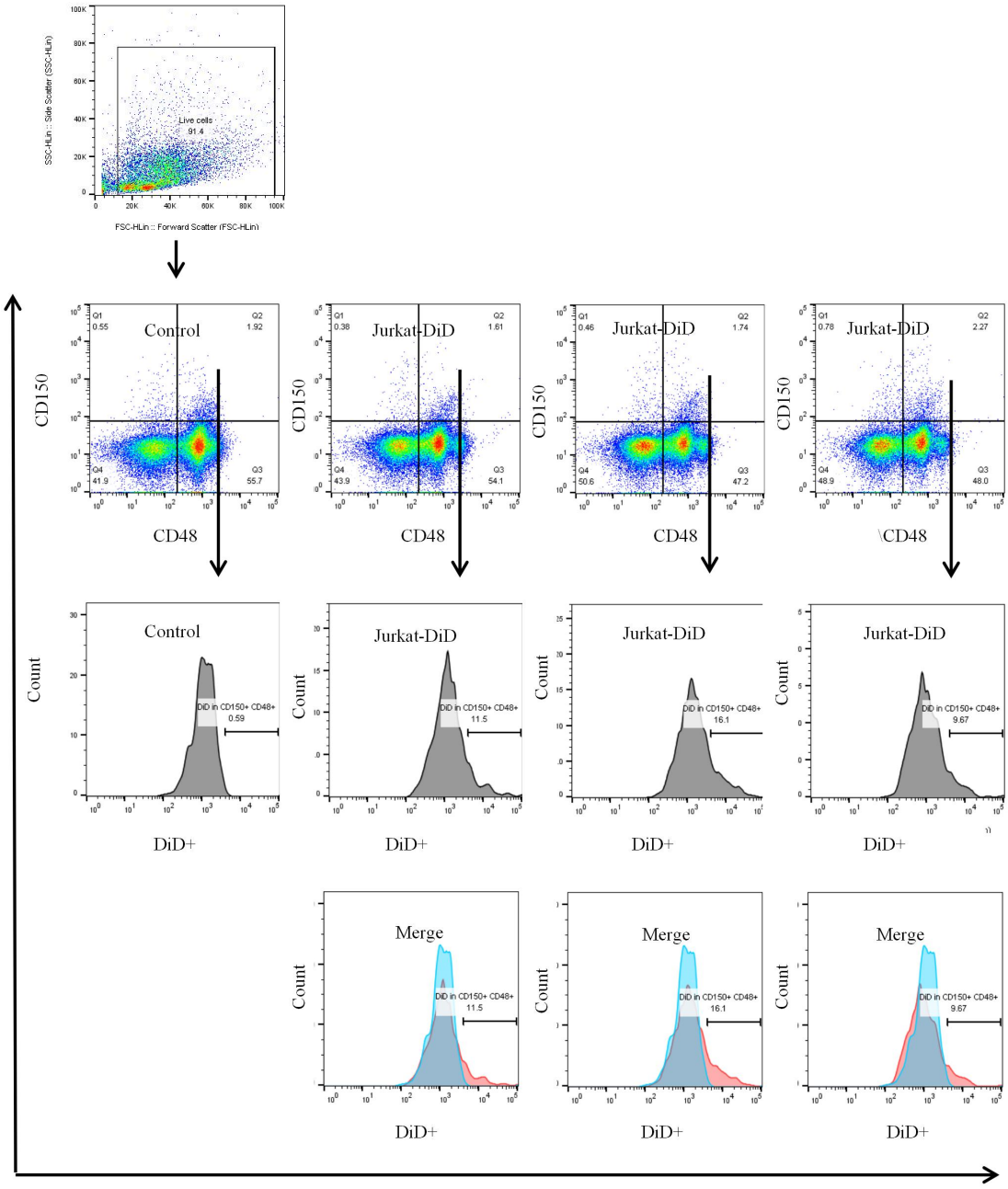

Supplemental Fig. S12: Gating strategy and identification of DiD positive hematopoietic progenitors 2 in BM. Please see Fig. S10 for details. The data are from 3mice.

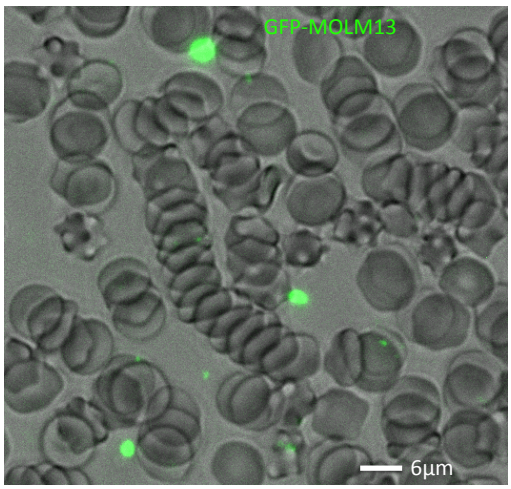

Supplemental Fig. S13: Subcellular size microparticles in blood 1 min post injection of GFP-MOLM13 cells in NSG mice. Only a few intact cells were detected per slide (n=2 mice).

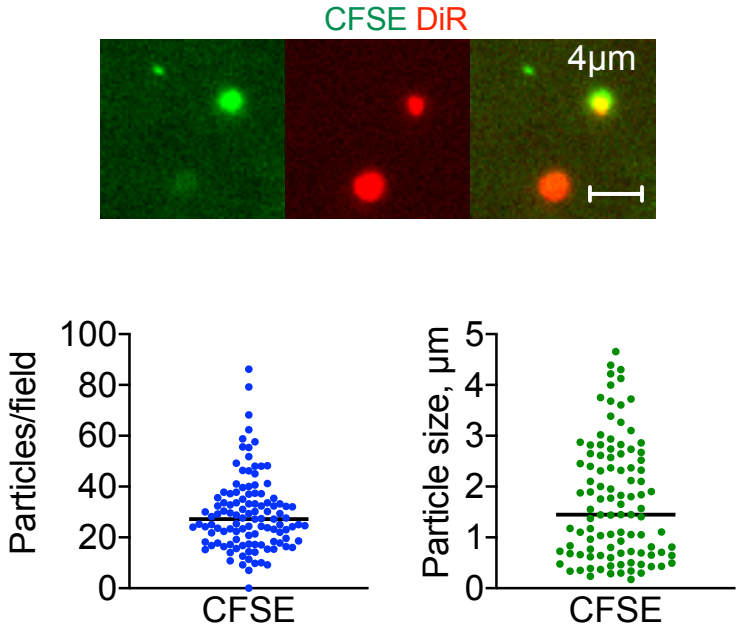

Supplemental Fig. S14: Splenocytes labeled with 25µM DiR and 10µM CFSE show microparticles in blood 1 min post injection in BALB/c mice (n=2 mice).

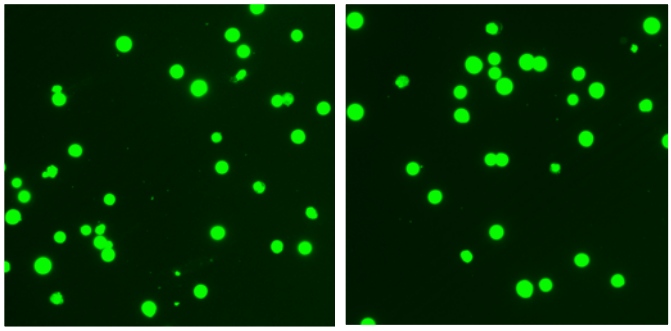

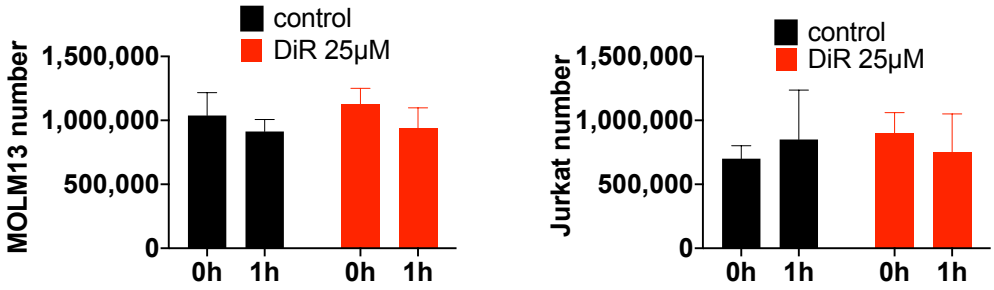

Supplemental Fig S15: Upper panel: incubation of CFSE-labeled Jurkat in BALB/c serum does not cause cell fragmentation. Cells were incubated in serum for 30 min at 37°C in the presence (left) or absence (right) of 10mM EDTA (complement inhibitor of all pathways). Lower panel: incubation of MOLM13 cells or Jurkat cells in BALB/c serum did not change the number of cells, excluding the complement-dependent lysis.

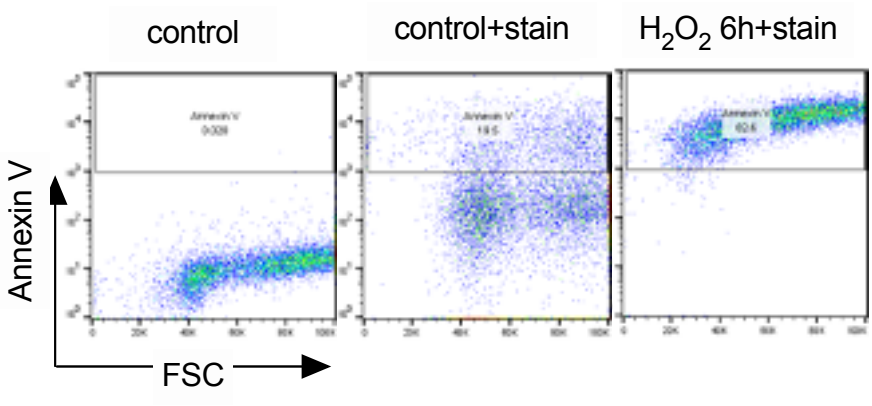

Supplemental Fig. S16. Apoptosis staining of DiR labeled Jurkat cells. Positive control cells were treated for 6h with hydrogen peroxide 500µM to induce apoptosis and stained with FITC-Annexin V. About 19% of non-peroxide treated Jurkat cells were apoptotic.

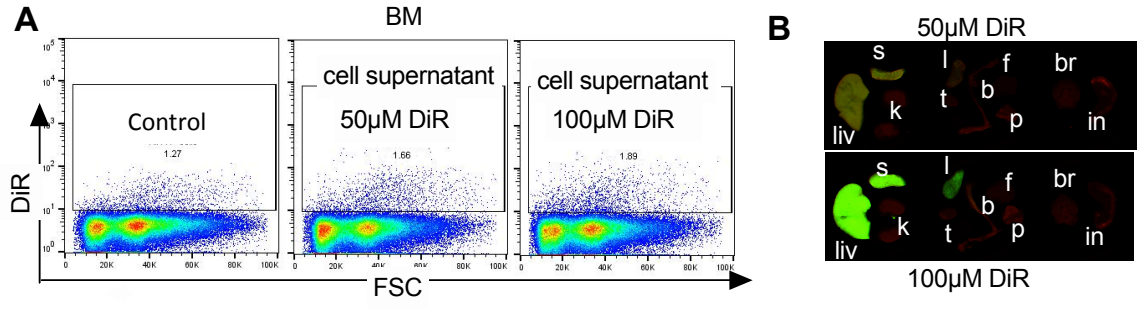

Supplemental Fig. S17: Supernatant was purified from 50 µM or 100 µM labeled DiR Jurkat cells by centrifugation at 400g for 2 min. **A**) flow cytometry and **B**) ex vivo NIR imaging 24h post injection showed minimal accumulation in the BM, suggesting that the residual free DiR do not contribute to the BM accumulation. Organ labels as in Fig. 1.

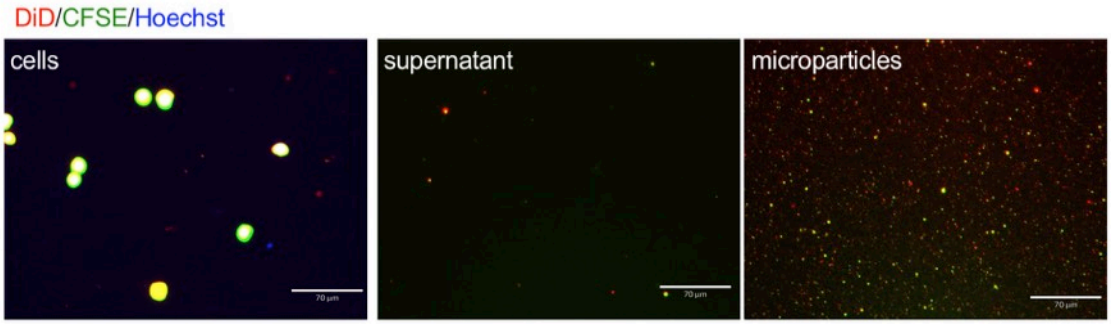

Supplemental Fig. S18: Jurkat cells were labeled with CFSE and DiD. Sonicated cells resulted in a much higher concentration of microparticles than in intact cells and cell supernatant (separated from cells at 400g for 2 min).